DOI:10.1190/image2022-3745669.1

Vz denoise and P/Z matching in 3D curvelet domain

Yong Ren, Chenhao Yang, Tim Seher, Matt Hawke and Eddie Cho (TGS)*

Summary

Ocean bottom node (OBN) seismic data processing commonly uses the combination of hydrophone (P) and vertical geophone (Z) components to separate upgoing and downgoing wavefields while attenuating ghosts and multiples. Because the vertical components are often contaminated by strong converted shear waves due to the scattering in the shallow subsurface, a good Vz noise removal is crucial for better P/Z calibration, wavefield separation and deconvolution. Most importantly, a better wavefield separation will in turn improve the quality of the seismic images. This paper will present a novel method of simultaneous Vz noise attenuation and P/Z calibration in the 3D curvelet domain. Furthermore, we will demonstrate that our new 3D method outperforms a 2-pass 2D curvelet approach. We will also assess the effect and necessity of Vz attenuation prior to shot carpet regularization. Both investigations are supported by field data examples from the Utsira OBN project.

Introduction

Up-down wavefield separation prior to deghosting and demultiple is a crucial step in OBN seismic data processing for achieving broadband, high quality seismic images. A typical workflow consists of P/Z calibration and up-down separation in the Tau-p domain (*Soubaras*, 1996), followed by up/down deconvolution (*Amundsen*, 1993; *Ziolkowski et al*., 1999; *Seher et al*., 2022). However, this method faces two challenges. The first challenge is that the up/down deconvolution is dependent of the data quality, as well as an accurate P/Z calibration. Both conditions could be easily compromised in OBN data since the vertical geophone can be severely contaminated with shear wave noise (*Paffenholz et al.*, 2006a, 2006b). Without proper Vz noise attenuation, P/Z calibration will not be accurate, and this will subsequently affect the up/down deconvolution. The second challenge is that current up/down deconvolution method assumes the subsurface being horizontally layered or with simple structures, and the approach will break down in the presence of complex structural geology. This challenge may be addressed with more recent method such as the multidimensional wavefield deconvolution (*Amundsen*, 2020).

A common method for Vz noise removal uses the P component which is mostly shear wave noise free to guide the denoising on the Z component. For this method to be efficient, one needs to use a sparse representation of the data. *Craft and Paffenholz* (2007) looked at the problem in Tau-p domain using a method of envelope ratio scaling between P and Z components for simultaneous geophone noise attenuation and up-down wavefield separation. *Ren et al.* (2020) used a P/Z amplitude ratio thresholding approach for Vz denoising in dual-tree complex wavelet domain. *Yang et al* (2020) proposed similar approach, but for both Vz denoise and P/Z matching in the 2D curvelet domain. They demonstrated that an efficient and accurate simultaneous Vz denoise and P/Z matching could be achieved in the curvelet domain, and the method overcomes the previously stated challenges.

In this paper, we will extend the approach proposed by *Yang et al.* (2020) which was limited to the 2D curvelet domain, to the 3D curvelet domain. We will demonstrate the effectiveness of our approach through testing on a real OBN dataset. We will compare the 2D curvelet and 3D curvelet methods and assess the impact on the OBN processing workflow.

Method and Workflows

Vz noise on the vertical geophone data is usually strong and stands out from the background signal. When analyzing the data in the curvelet domain, which has the advantage of promoting the sparsity, the noise can be easily distinguished from the signal when comparing P and Z components. Here, we use the 3D curvelet transform developed by *Candes et al.* (2006) to decompose the data into this domain with different scales and dips for an efficient simultaneous Vz noise attenuation and P/Z matching.

Vz denoise and P/Z matching in 3D curvelet domain

Following are the main steps of our approach:

1) 3D curvelet transform of P and Z components.
2) Application of a scale and orientation-dependent thresholding process on the P/Z amplitude ratio targeting the Vz noise attenuation as shown in following equation:

$$\tilde{V}_z = \begin{cases} V_z, & r \geq \alpha \\ 0, & r < \alpha \end{cases}$$

where r is the P/Z amplitude ratio, α is the thresholding value and $\tilde{V}_z$ is the denoised Vz component in the curvelet domain.

3) Application of P/Z envelope matching on each of the curvelet coefficients. This process will also further attenuate the Vz noise. The P/Z envelope ratio that is used to scale each Vz curvelet coefficient, is formulated as following:

$$C(s,d,t,x) = \frac{|P(s,d,t,x)|}{|Z(s,d,t,x)|}$$

where s and d are scales and dip angles in the curvelet domain, t and x are time and spatial coordinates.

4) Inverse 3D curvelet transform for the matched Vz component.

Once the Vz component has been denoised and matched, the hydrophone and geophone can be combined to separate the upgoing and downgoing wavefields through a simple summation.

Considering the high demand on computation and memory for the 3D curvelet transform, we divided the full volume of a receiver gather into overlapping 3D sub-volumes and applied our 3D curvelet method to each of them.

Workflows

In this paper, we use 3D curvelet domain Vz denoise and P/Z matching to assess different steps in the processing workflow. Figure 1 shows different workflows used in this study. In the first set of tests, we will use the workflows to investigate the comparison between the 2D curvelet and 3D curvelet methods. Before applying the Vz denoise and P/Z matching step, P and Vz components have been regularized without any prior Vz denoise. In the second set of tests, we will focus on the effect of a one pass 2D Vz denoise prior to the shot carpet regularization in our method.

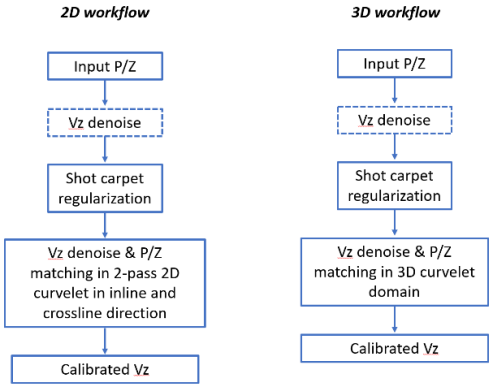

Figure 1: Different workflows for Vz denoise and Vz matching in 3D curvelet domain. The first Vz denoise step (dashed lines) is optional.

Results

We have applied our processing workflows on real data from the Utsira OBN survey acquired in the North Sea. The survey was acquired in 2018 and 2019 using 2-3 vessels with triple sources shooting. The shot spacing is 25 m and the distance between two shot lines is about 50m. After shot carpet regularization, the distance in both directions becomes 12.5 m. Figure 2 shows an example of P and Z components depicting strong Vz noise on the Z component.

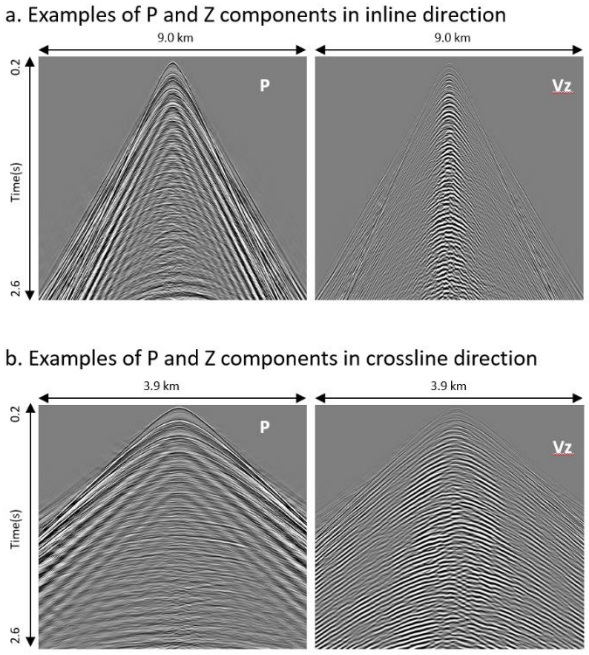

Figure 2: Examples of P and Z components of Utsira data for the inline direction (a) and the crossline direction (b).

In the following section, we will discuss two comparisons:

1) Curvelet domain method for 2D and 3D approaches.

2) Comparison of results from the workflows with and without a one-pass 2D Vz denoise before the shot carpet regularization.

Comparison 2D/3D curvelet domain

For the comparison between 2D and 3D curvelet methods, we have applied shot carpet regularization of P and Z components with and without prior Vz denoise. For the 2D curvelet workflow we have applied a first pass of 2D curvelet Vz denoise and P/Z matching in the inline direction followed by another pass along the crossline direction (Figure 1, left). For 3D workflow, the shot carpet regularization is followed by only one 3D curvelet Vz denoise and P/Z matching (Figure 1, right). The comparison of our results for both cases with and without prior Vz denoise has come to the same conclusion, therefore we will

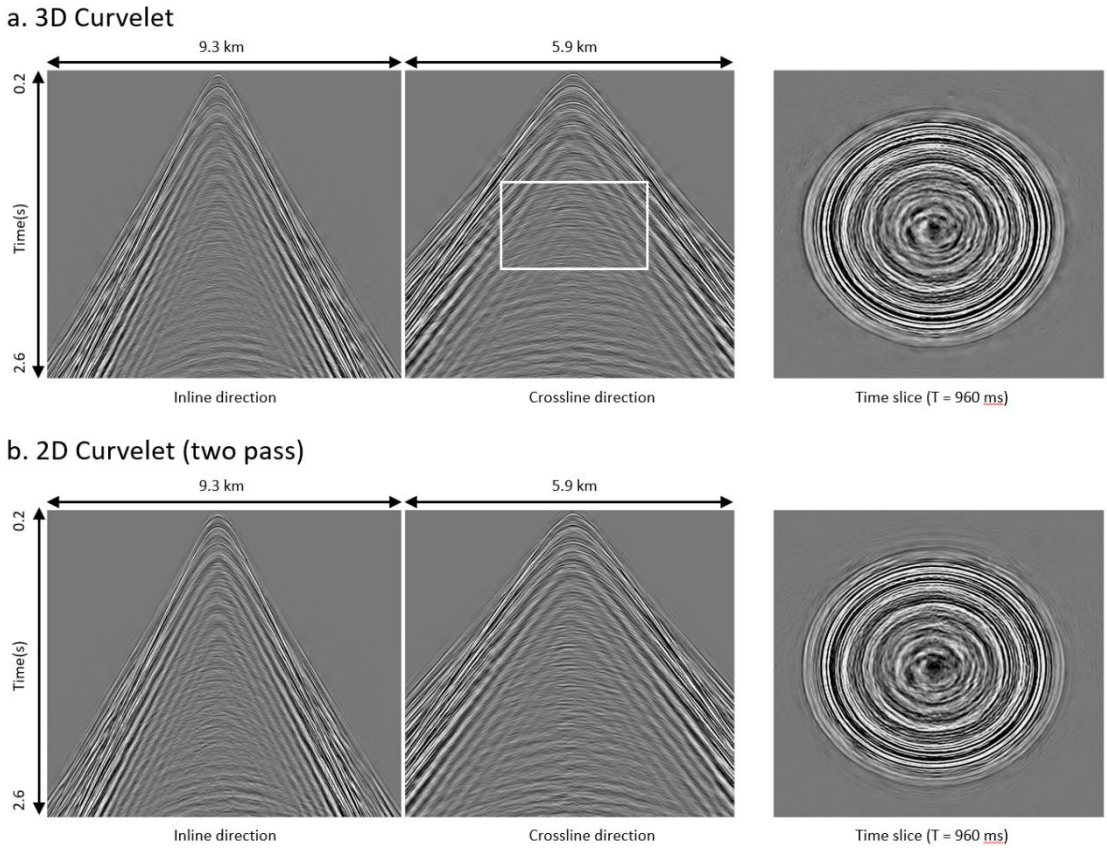

Figure 3: Comparison of 3D curvelet matching and two-pass 2D curvelet matching on regularized P and Vz data. a). 3D curvelet: matched Vz for for the inline direction (left), the crossline direction (middle) and the time slice at 960 ms (right). b). 2D curvelet: matched Vz for for the inline direction (left), the crossline direction (middle) and the time slice at 960 ms (right).

show in this paper only the results for the case without the prior Vz denoise.

Figure 3 shows a comparison of results between simultaneous Vz denoise and P/Z matching in the 3D curvelet domain and with a two-pass 2D curvelet transform. The first observation of the results shows that both the 3D curvelet and 2D curvelet methods performed well in terms of Vz denoise and P/Z matching. However, the 3D curvelet approach still brings some improvements. For instance, at shallow regions, less artefacts can be observed from the 3D curvelet. The events after denoise and matching look much more coherent compared to the 2D curvelet results, shown on the time slices in Figure 3. Furthermore, the advantage of the 3D curvelet method is particularly noticeable in the crossline direction when compared with the 2D method. The use of scales and dip information made possible in the 3D implementation allows a better suppression of the shear wave noise and significantly improves the continuity of the events as illustrated in Figure 4, showing a zoomed area along the crossline direction.

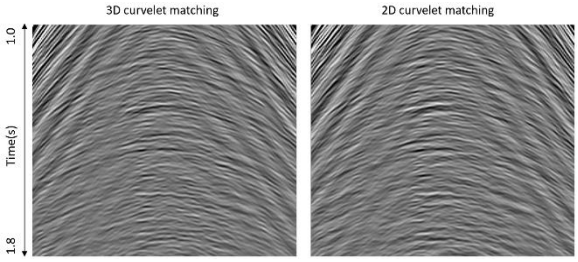

Figure 4: Comparison of 3D curvelet Vz matching and two-pass 2D curvelet matching for regularized data along crossline direction (for a zoomed area see figure 3). Left: 3D curvelet. Right: two-pass 2D curvelet.

Vz denoise before and after regularization

Shear wave noise present on the vertical geophone can be very strong and a step of Vz denoise preprocessing should usually be carried out before the P/Z matching. In this section, we will investigate the effect and necessity of such a step in our 3D workflow shown in Figure 1, right. In one case, we have applied a one-pass 2D curvelet Vz denoise

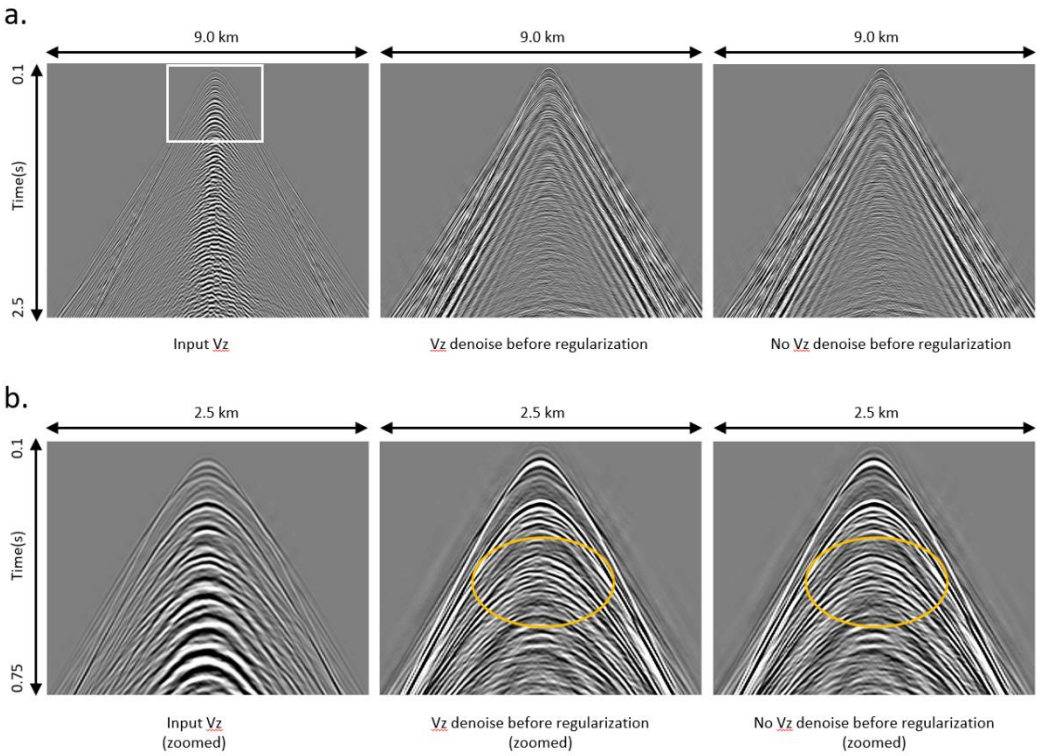

Figure 5: Comparison of results for 3D curvelet P/Z matching on regularized P and Vz component with and without a 2D Vz denoise prior regularization. (a): Example of a Vz component before P/Z matching (left); matched Vz component with a 2D one-pass Vz denoise before regularization and matched Vz component without any Vz denoise before regularization (right). b): Same as a) for a zoomed area (white rectangle).

before the shot carpet regularization, and in another case, we omit this step prior to the regularization. The 3D curvelet Vz denoise and P/Z matching is then applied after the regularization in both cases. Figure 5 shows the results of the application of the two workflows for an example receiver gather. As illustrated in Figure 5a, we first notice that both workflows produce overall very similar results, where the Vz noise has been nicely attenuated and matched to P. However, if we look at the results more closely, in some areas the workflow without the 2D Vz denoise prior to regularization produced a better continuity of events (as depicted by yellow ellipses in Figure 5b). This observation is only preliminary, and some further testing is needed. However, we can at least conclude that the workflow without a prior Vz denoise step before the regularization produced a result of same quality as the workflow with that step. This means that the 2D Vz denoise step before regularization is not necessary in our approach, which is important as it will simplify the processing workflows and save processor time.

Conclusions

We have presented a method of simultaneous Vz attenuation for vertical geophones and P/Z matching in the 3D curvelet domain. The application of our approach on a real OBN dataset has demonstrated that our 3D curvelet method outperforms a two-pass 2D curvelet method in preserving the continuity of events on the Z component when matched to the P component. In our other tests, we also showed that it may not be necessary to apply 2D Vz denoise before the shot carpet regularization in our 3D curvelet denoise and matching method workflow. On the contrary, preliminary results show that our 3D curvelet approach can sometimes perform even better without the pre-regularization denoise step. Our method permits a high quality up/down wavefield separation, while at the same time provides a great improvement in the processing workflow in terms of simplicity and computation time.

Acknowledgments

We would like to thank TGS management for permission to show the Utsira OBN data, which was acquired in partnership with Axxis Multi-Client. We appreciate all the helpful technical discussions from Yu Zhou, Zhaojun Liu, Carsten Udengaard and Hassan Masoomzadeh. We also would like to thank Sarah Spoors, Adriana Citlali Ramirez and Mikal Trulsvik for their helpful reviews and comments.

References

Amundsen, L., 1993, Wavenumber-based filtering of marine point-source data: Geophysics, **58**, no. 9, 1335–1348, doi: https://doi.org/10.1190/1.1443516.

Amundsen, L., 2020, Review of up-down deconvolution and multidimensional deconvolution for designature/free-surface demultiple of OBN seismic data: SEG International Exposition and 90th Annual Meeting, Expanded Abstracts, 3093–3098, doi: https://doi.org/10.1190/segam2020-3417830.1.

Candès, E., L. Demanet, D. L. Donoho, and L. Ying, 2006, Fast discrete curvelet transforms: Multiscale Modeling and Simulation, **5**, no. 3, 861–899, doi: https://doi.org/10.1137/05064182X.

Craft, K., and J. Paffenholz, 2007, Geophone noise attenuation and wavefield separation using multidimensional decomposition technique: 77th Annual International Meeting, SEG, Expanded Abstracts, 2630–2634, doi: https://doi.org/10.1190/1.2793013.

Paffenholz, J., R. Shurtleff, D. Hays, and P. Docherty, 2006a, Shear wave noise on OBS Vz data — Part I evidence from the field: 68th Annual International Conference and Exhibition, EAGE, Extended Abstracts, B046, doi: https://doi.org/10.3997/2214-4609.201402227.

Paffenholz, J., P. Docherty, R. Shurtleff, and D. Hays, 2006b, Shear wave noise on OBS Vz data-Part II elastic modeling of scatterers in the seabed: 68th Conference and Exhibition, EAGE, Extended Abstracts, B047, doi: https://doi.org/10.3997/2214-4609.201402228.

Ren, Y., C. Yang, T. Degel, and Z. Liu, 2020, Vz noise attenuation using dual-tree complex wavelet transform: SEG International Exposition and 90th Annual Meeting, Expanded Abstracts, 1830–1834, doi: https://doi.org/10.1190/segam2020-3426428.1.

Seher, T., Y. Ren, H. Masoomzadeh, T. Degel, E. Cho, M. Hawke, and S. Baldock, 2022, Deconvolution of upgoing and downgoing wavefields: A data example from the Utsira OBN survey: 83nd EAGE Annual Conference and Exhibition, Extended Abstracts, 1–5.

Soubaras, R., 1996, Ocean bottom hydrophone and geophone processing: 66th Annual International Meeting, SEG, Expanded Abstracts, 24–27, doi: https://doi.org/10.1190/1.1826611.

Yang, C., Y. Huang, Z. Liu, J. Sheng, and E. Camarda, 2020, Shear wave noise attenuation and wavefield separation in curvelet domain: SEG International Exposition and 90th Annual Meeting, Expanded Abstracts, 1805–1809, doi: https://doi.org/10.1190/segam2020-3426418.1.

Ziolkowski, A. M., D. B. Taylor, and R. G. K. Johnston, 1999, Marine seismic wavefield measurement to remove sea-surface multiples: Marine seismic wavefield measurement: Geophysical Prospecting, **47**, no. 6, 841–870, doi: https://doi.org/10.1046/j.1365-2478.1999.00165.x.